Enhanced copper micro/nano-particle mixed paste sintered at low temperature for 3D interconnects

Y. Y. Dai,[1,2] M. Z. Ng,[2,3] P. Anantha,[1,2] Y. D. Lin,[1] Z. G. Li,[2,3] C. L. Gan,[2,3] and C. S. Tan[1,2,a)]
[1]*School of Electrical and Electronic Engineering, Nanyang Technological University, 50 Nanyang Avenue, Singapore 639798*
[2]*NTU-Lockheed Martin Joint Lab, Nanyang Technological University, Research Techno Plaza, 50 Nanyang Drive, Singapore 637553*
[3]*School of Materials Science and Engineering, Nanyang Technological University, 50 Nanyang Avenue, Singapore 639798*

(Received 28 April 2016; accepted 11 June 2016; published online 27 June 2016)

An enhanced copper paste, formulated by copper micro- and nano-particles mixture, is reported to prevent paste cracking and obtain an improved packing density. The particle mixture of two different sizes enables reduction in porosity of the micro-paste and resolves the cracking issue in the nano-paste. *In-situ* temperature and resistance measurements indicate that the mixed paste has a lower densification temperature. Electrical study also shows a ~12× lower sheet resistance of 0.27 Ω/sq. In addition, scanning electron microscope image analysis confirms a ~50% lower porosity, which is consistent with the thermal and electrical results. The 3:1 (micro:nano, wt. %) mixed paste is found to have the strongest synergistic effect. This phenomenon is discussed further. Consequently, the mixed paste is a promising material for potential low temperature 3D interconnects fabrication. *Published by AIP Publishing*. [http://dx.doi.org/10.1063/1.4954966]

Three-dimensional integrated circuits (3D IC) draw much attention in recent years as they offer a promising way for enhanced performance and efficient integration due to vertical stacking.[1] Low temperature metal-metal bonding is an important enabler for 3D IC technologies for applications in various electronics products.[2,3] At present, Cu-Cu bonding receives significant interest both in academic research and industrial development because copper has excellent electrical and thermal conductivities as well as electro-migration resistance.[4] Most importantly, it is widely used in electronic manufacturing and is often considered as a low cost solution.[5–7]

Researchers are attempting to lower the Cu-Cu bonding temperature via surface passivation or balancing the pressure and temperature during thermo-compression bonding.[8] However, this increases either the process complexity or the risk of damage when devices undergo high mechanical pressure. In addition, when the process temperature is higher than desired, the material would weaken and this can lead to failure.[9] Therefore, bonding assisted with metallic particles paste is proposed as an efficient method to solve the metal-metal bonding issues.

Metallic particles have large surface area to volume ratio as well as high surface energy, thus offering lower temperature required during bonding.[10] Besides, metallic particles can endure temperatures higher than their melting point by converting to the bulk state.[9] Thus, various aspects of copper nanoparticles paste used for interconnects formation are actively studied as reported by Tan and Cheong[11] and Yamakawa *et al.*[12] However, several studies have consistently reported the issue of mechanical cracking in the joints formed by copper nanoparticles paste which results in low bond strength and reliability.[13,14]

Cracks persist during paste drying partly because of the densification stress imposed by solvents evaporation. Soft particles tend to deform and form pores, while hard particles develop cracks to release stress.[15] Nano-suspension are prone to nucleation cracking and the reason for that is more complicated.[16] Additionally, nanoparticles always present a much higher cost due to its delicate synthesis process which may render them unsuitable for mass industrial production.[4] Hence, we study and develop a method of mixing copper micro-particles with copper nano-particles in an attempt to improve the paste packing density and to further enhance the paste quality. The micro-particles could prohibit cracks in nano-particle paste due to their large size; the nanoparticles in return are able to fill the interstitial space between the micro-particles. In this way, the mixed paste could resolve the limitations imposed by both micro- and nano-particles paste. Since the required amount of nano-particles is smaller in the mixed paste, the overall cost is expected to reduce. It is found that the mixed paste with a ratio of 3:1 (micro:nano, wt. %) provides the best performance. This letter shows the improvements achieved in the mixed paste in terms of packing density, thermal, electrical, and mechanical properties.

Copper micro-particles are purchased from commercial supplier (American Elements, 1–2 μm in diameter, 99% purity). The copper nano-particles are received from Lockheed Martin Advanced Technology Center (40–60 nm in diameter, surface passivated).[17] IPA (3-Indolepropionic acid) is added to disperse copper particles with the same amount in each kind of paste. To obtain a uniformly mixed paste, the micro- and nano-paste were mixed together using a homogenizer (Heidolph, SilentCrusher M). The copper micro-particles are assumed to have a Face Centered Cubic (FCC) arrangement with a ~74% packing density, while the remaining ~26% space is to be occupied by nano-particles. Therefore, the

a)Electronic mail: tancs@ntu.edu.sg.

mixed paste was first made with a ratio of 3:1 (micro:nano, wt. %; all the ratios mentioned herewith are in this sequence). For the purpose of benchmarking, samples consisting of only micro-particles or only nano-particles were also prepared for comparison.

Paste application on the glass substrate was carried out using the doctor blade technique to form a film. *In-situ* resistance and temperature measurements were carried out using a tube furnace. It is connected with a current generator to measure the densification temperature and change in resistance during sintering. A thermocouple was used to monitor the furnace temperature. This set-up is used to obtain the paste sintering profile. An area of 1 mm × 1 mm square on the applied film is chosen for measurement. Sheet resistance was measured to investigate the paste electrical property using the Sheet Resistance Measurement System (CMT-SR2000N). Paste packing density was characterized by porosity estimated from Scanning Electron Microscope (LEO 1550 Gemini, SEM) images using color contrast estimation with ImageJ software. All the sintering processes conducted in this study are the same: 230 °C for 10 min in N_2, with a ramping rate of 20.5 °C/min. The paste was dried before curing.

Figure 1 shows the evolution of the *in-situ* resistance of the three types of paste during sintering. For the first 10 min, the temperature ramps up from room temperature to 230 °C. Thus, the critical temperature of the paste can be identified from Figure 1, which is corresponding to the time when the resistance shows an abrupt decrease. The pastes have high resistance before sintering. This may be caused by the protective layer leading to poor conduction[18] and the segregation of these particles. Solvents and additives remain in the fresh paste also aggravate resistance. During temperature ramping stage, the mixed paste displays a dramatic resistance decrease first followed next by the micro-paste and nano-paste. When the paste resistance decreases to below 10 Ω, there is no further change in the resistance indicating that the particles are well fused. This is often accomplished with the evaporation of most of the solvent and protective layer. The temperature at this stage is the densification temperature which is observed at 150, 220, and 140 °C for the micro-, nano-, and mixed paste, respectively. The lowest densification temperature of the mixed paste indicates that the mixture is more compact allowing for uniform heat distribution during sintering or the solvent evaporates earlier. This enables the particles to fuse well at low temperature. Since the micro-particles are handled to remove the surface oxide prior to paste formulation, the protective layer could volatilize readily. This could be the reason which leads to their lower densification temperature in micro-paste as compared to the nano-paste.

During the final stage of the sintering process, the nano-paste shows an interesting phenomenon where the resistance initially decreases gradually to 1.8 Ω and then suddenly increases to 50 kΩ (at 14th minute). During sintering, cracks form due to the shrinkage of the film as a result of solvents evaporation.[19–21] The difference in solvents' evaporation rates causes the film to be stressed and eventually crack. We speculate that these cracks occur in the nano-paste as well, causing an abrupt change in the resistance. Since these cracks are permanent, the increase in the resistance is irreversible.

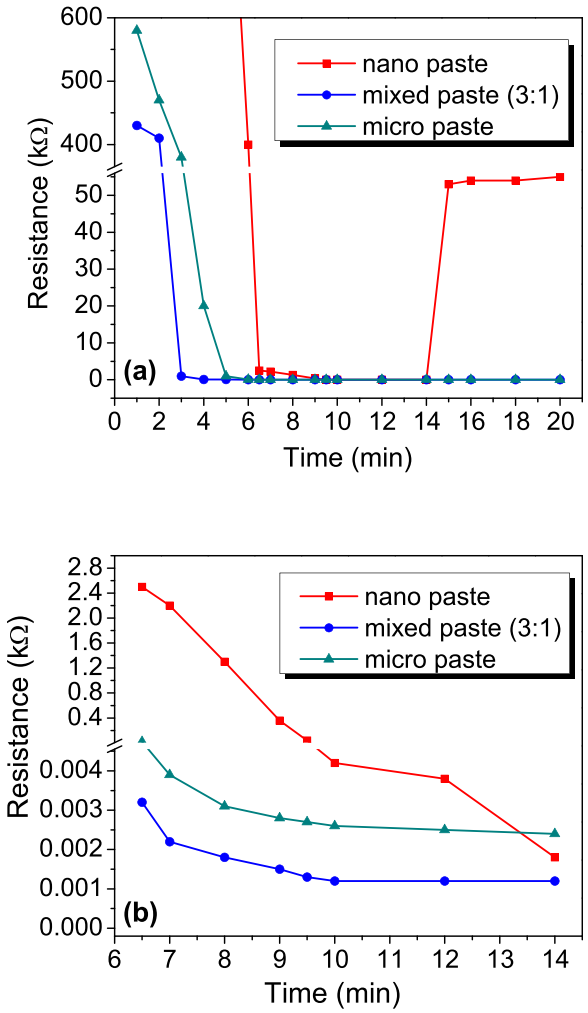

FIG. 1. (a) *In-situ* resistance change of micro-, nano-, and mixed paste. (b) Resistance change between 6th and 14th min. Temperature ramps up from room temperature to 230 °C in the first 10 min and remains at 230 °C for sintering in the subsequent 10 min.

Figure 1(b) shows a clear resistance change between 6th and 14th min. After sintering, the mixed paste has the lowest resistance, and the specific results are listed in Table I for comparison. However, the resistance tested by this measurement is sensitive to thickness variation, and therefore, a four-point-probe is subsequently utilized to accurately investigate the electrical property.

Figure 2(a) shows the sheet resistance results of nano-, micro-, and mixed pastes after sintering. The nano-paste has a large resistance range at a high mean value. The challenges faced while measuring the sheet resistance indicate the existence of large macrosized brittle failures in the sintered paste surface. This is also an indirect indication that cracks occur in the nano-paste during the sintering process, as the mixed and micro-paste do not present such an abnormality. The

TABLE I. *In-situ* resistance and temperature results comparison.

Paste	Densification temperature	Resistance after sintering	Crack
Micro-paste	150 °C	2.3 Ω	No
Nano-paste	220 °C	1.8 Ω	Yes
Mixed paste	140 °C	1.0 Ω	No

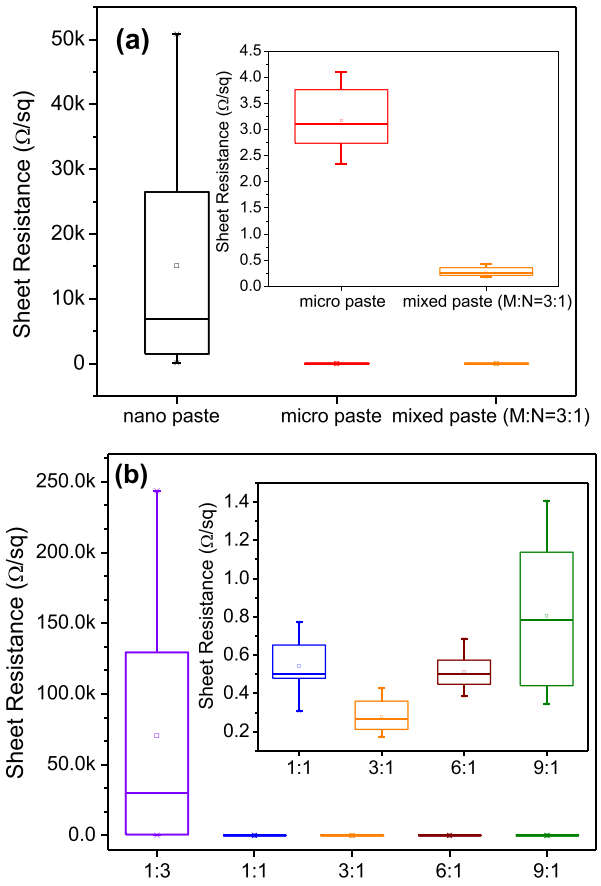

FIG. 2. Sheet resistance of (a) nano-, micro-, and mixed paste (3:1). Inset: comparison of micro-paste and mixed paste and (b) mixed paste with different ratios. Inset: comparison of 1:1, 3:1, 6:1, and 9:1 mixed paste.

average sheet resistance of the micro-paste is 3.2 Ω/sq while that of mixed paste is only 0.27 Ω/sq on average. The higher conductivity is likely attributed to the high packing density of the mixture which ensures high connectivity of the particles. To further determine the optimal mixing ratio, pastes with several other ratios are prepared and characterized. Figure 2(b) shows that the 1:3 (micro:nano) paste sheet resistance is still out of the normal range. It is probably because the small amount of microparticles are not sufficient to significantly alter the properties of the nanoparticle rich paste. The results of the other pastes fall within the normal range, and the inset image shows the detailed comparison. The 3:1 (micro:nano) paste has the lowest sheet resistance as expected, whereas 9:1 has the highest value which may correspond to the large porosity caused by the insufficient quantity of nano-particles to fill the interstitial of the micro-particles.

The samples are then inspected with scanning electron microscopy (SEM). SEM images are utilized for visual analysis in order to observe the porosity of different types of paste and also to verify if the cracks occur in the nano- and 1:3 mixed pastes. Figures 3(a) and 3(b) show the surface morphology of micro- and nano- paste, respectively. The micro-paste displays large visible porous regions whereas clear cracks are seen on the nano-paste surface. The 1:3 paste also presents small cracks, but the 1:1 paste shows some improvements with much reduced brittle cracks with a 22.1% porosity as compared to the 27.8% in the micro-paste. The incomplete sintering of the micro-particles may cause large porosity. In terms of crack formation in the nano-paste, apart from the evaporation rate differences, a high evaporation loss is also a possible reason. This leads to a drying crack formation during curing.

The images of the pastes in which the micro-particles have a higher ratio than the nano-particles are shown in Figure 4. The 3:1 paste is the most compact with a porosity of only 13.6%. Due to the lack of nano-particles, the 9:1 paste is highly porous similar to the micro-paste with a high porosity (Fig. 3(a)). The SEM images verify the preceding crack formation hypothesis as discussed above and give the

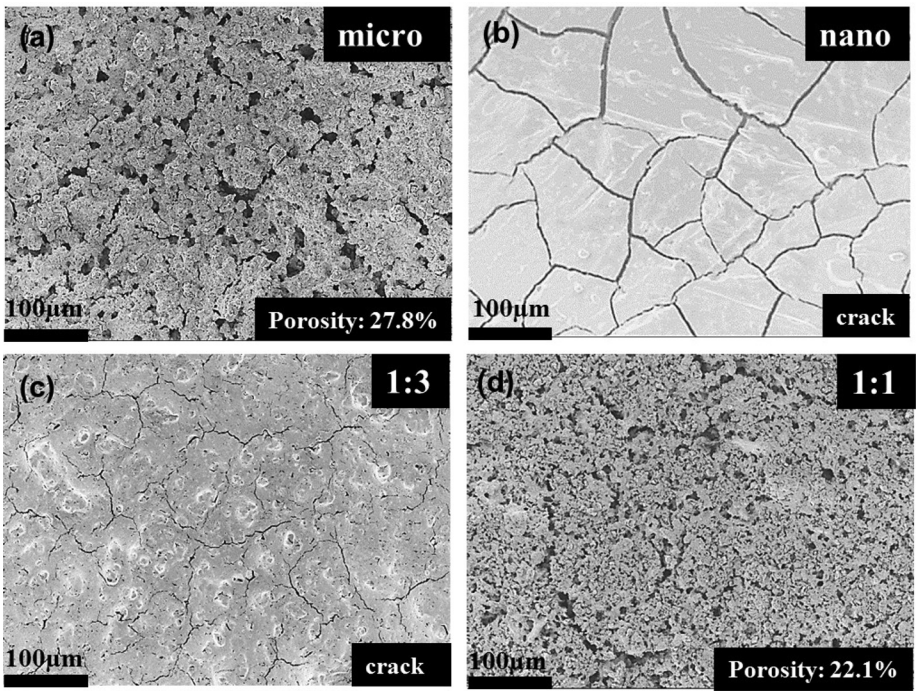

FIG. 3. SEM images (top-view) of (a) micro-paste, (b) nano-paste, (c) 1:3 (micro:nano) mixed paste, and (d) 1:1 (micro:nano) mixed paste; porosity is calculated by ImageJ image analysis software.

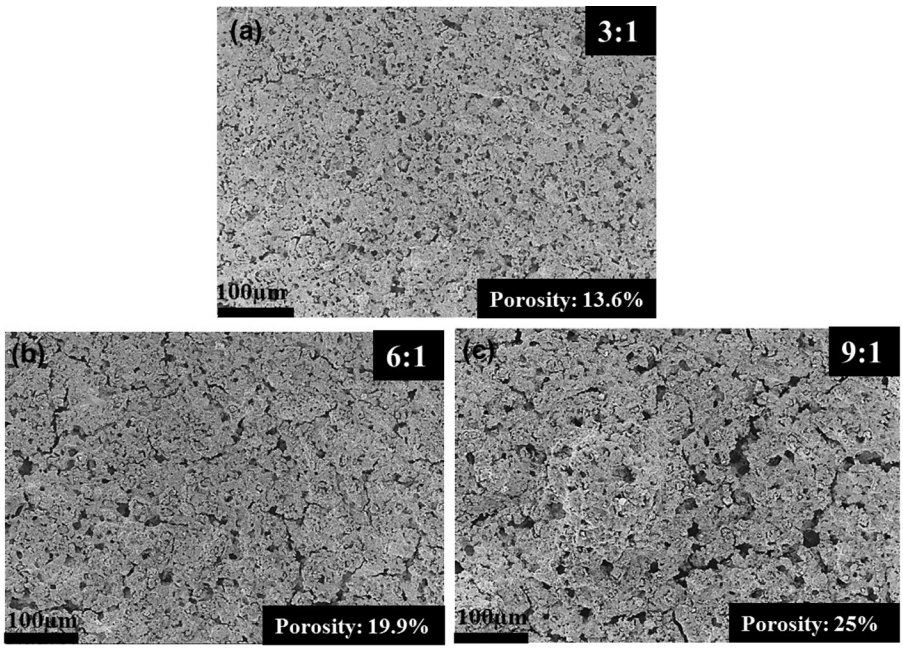

FIG. 4. SEM images (top-view) of (a) 3:1 (micro:nano) mixed paste, (b) 6:1 mixed paste, and (c) 9:1 mixed paste.

specific packing density results which are consistent with the thermal and electrical characterizations.

Afterwards, we conducted die to wafer bonding to examine the copper particles paste mechanical reliability when they are put into practical use. The die size is 5 mm × 5 mm, and the substrate size is 2.5 cm × 2.5 cm. Both the silicon die and wafer are sputtered with 50 nm Ti barrier layer and 500 nm Cu layer prior to bonding. Bonding was accomplished pressure-free in N_2 atmosphere at 200 °C, as targeted for low temperature application, for 20 min and is allowed to cool down naturally. Subsequently, the bonded dies were subject to the shear test and the results are shown in Figure 5. An average shear bond strength of 0.7 MPa is achieved for the mixed paste, which is higher than that of micro- and nano-paste. This outcome agrees with the thermal and electrical characteristics. Therefore, the mixed paste could be used in Cu-Cu bonding such as Cu pillar to landing pad bonding with a paste thickness in the range of 5–10 μm for low temperature micro-joints application.

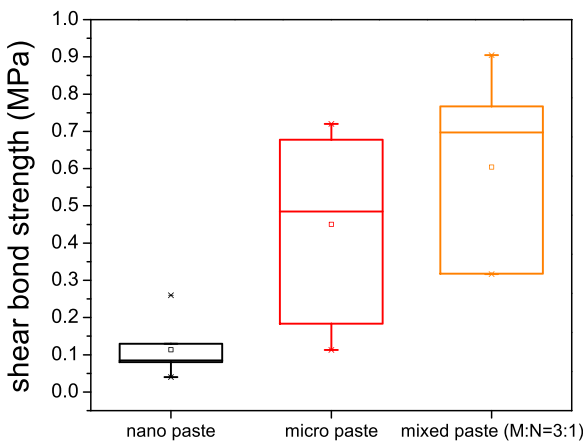

FIG. 5. Shear bond strength of nano-, micro-, and mixed paste; bonding condition is pressure-free 20 min in N_2 atmosphere at 200 °C, with ramping rate of 17 °C/min.

To understand the fundamental physics of the synergistic effect of micro- and nano-particles during sintering and reason for the crack formation in nano-paste, we analysed the failure mode interface. It was found that samples bonded with micro- and mixed paste fractured between the particles whereas those with nano-paste was observed to break at the interface, which could be regarded as a brittle fracture. Therefore, the plastic-brittle transition should happen during nano-paste sintering. Due to smaller particle size, they may form bodies attracted by the weak Van der Waals force which is prone to exhibit a brittle transition.[22,23] When particles undergo the sintering process, the force between the particles could prevent cracks and inhibit particles separation.[24,25] Due to nano-particles agglomeration, this strength would decrease.[24] Hence, the nano-paste displays plastic-brittle fracture transition rather than simple voids. In addition, there is another parameter to evaluate the cracks distribution called the Peclet number, which is proportional to the particle radius. Experiments conducted by Yamamura *et al.* gives us a reference that paste with high Peclet number is less likely to have brittle crack.[26] In conclusion, the nano-paste shows high sinter activity but suffers from crack formation during drying at low temperature, while the micro-paste shows sufficient drying but they form only a low number of unstable sintering necks. Therefore, trading off between the paste packing density and particle size, which is in turn dependent on the mixture ratio, it becomes vital to get a paste with no-cracks and displaying an enhanced mechanical stability. Our experiments verified that the copper particle mixture ratio 3:1 (micro:nano) is suitable to obtain improved performance in actual experiment, consistent with theoretical reports.[27]

During the mixed paste sintering, the differential evaporation rate generates capillary stress to densify the paste. The protective layer of the micro-particles would first evaporate and then the particles begin to fuse. As the existing nano-particles cluster, the inter-particle attraction between particles

would be stronger and porosity decreases. In addition, high inter-particle potential link the nano-particles with micro-particles rapidly and reduce the resistance. Chemical bond formed between adjacent particles in this process is also a possible reason to improve the mixed paste mechanical property.[28,29] This could be further investigated for complete analysis.

In summary, the paste obtained by the 3:1 mixture of copper micro- and nano-particles exhibits more than 50% lower porosity as compared to micro-paste and no cracks are observed. It has a lower densification temperature of only 140 °C and is thus ideal for low temperature sintering for Cu-Cu micro-joint formation. In addition, an improvement in electrical conductivity is also shown with a sheet resistance of 0.27 Ω/sq, which is ∼12× lower than that of the micro-paste. Therefore, this mixed paste that consists the optimum ratio of copper micro-particles and nano-particles is a promising electronic material as 3D interconnects, highly suitable for low temperature joints, RFID (Radio Frequency Identification)[30] and bonding application.

This work was funded by a seed grant from TL@NTU. C. S. Tan is affiliated with Si-COE and NOVITAS in Nanyang Technological University.

[1]A. Kim, E. Choi, H. Son, and S. G. Pyo, J. Nanosci. Nanotechnol. **14**(2), 2001 (2014).
[2]A. Huffman, J. Lannon, M. Lueck, C. Gregory, and D. Temple, J. Instrum. **4**(03), P03006 (2009).
[3]A. Hu, J. Y. Guo, H. Alarifi, G. Patane, Y. Zhou, G. Compagnini, and C. X. Xu, Appl. Phys. Lett. **97**(15), 153117 (2010).
[4]T. Ishizaki, A. Kuno, A. Tane, M. Yanase, F. Osawa, T. Satoh, and Y. Yamada, Microelectron. Reliab. **54**(9), 1867 (2014).
[5]Y. S. Tang, Y. J. Chang, and K. N. Chen, Microelectron. Reliab. **52**(2), 312 (2012).
[6]C. S. Tan, D. F. Lim, S. G. Singh, S. K. Goulet, and M. Bergkvist, Appl. Phys. Lett. **95**(19), 192108 (2009).
[7]L. Peng, L. Zhang, J. Fan, H. Y. Li, D. F. Lim, and C. S. Tan, IEEE Electron Device Lett. **33**(12), 1747 (2012).
[8]C. T. Ko and K. N. Chen, Microelectron. Reliab. **52**(2), 302 (2012).
[9]Y. Kobayashi, Y. Abe, T. Maeda, Y. Yasuda, and T. Morita, J. Mater. Res. Technol. **3**(2), 114 (2014).
[10]T. G. Lei, J. N. Calata, G. Q. Lu, X. Chen, and S. Luo, IEEE Trans. Compon. Packag. Technol. **33**(1), 98 (2010).
[11]K. S. Tan and K. Y. Cheong, IEEE Trans. Compon., Packag., Manuf. Technol. **4**(1), 8 (2014).
[12]T. Yamakawa, T. Takemoto, M. Shimoda, H. Nishikawa, K. Shiokawa, and N. Terada, J. Electron. Mater. **42**(6), 1260 (2013).
[13]K. Schnabl, L. Wentlent, K. Mootoo, S. Khasawneh, A. A. Zinn, J. Beddow, E. Hauptfleisch, D. Blass, and P. Borgesen, J. Electron. Mater. **43**(12), 4515 (2014).
[14]J. Zurcher, K. Yu, G. Schlottig, M. Baum, M. M. Visser Taklo, B. Wunderle, P. Warszynski, and T. Brunschwiler, in *Proceedings of the IEEE 65th Electronic Components and Technology Conference* (2015), p. 1115.
[15]K. B. Singh and M. S. Tirumkudulu, Phys. Rev. Lett. **98**(21), 218302 (2007).
[16]P. Xu, A. S. Mujumdar, and B. Yu, Drying Technol. **27**(5), 636 (2009).
[17]A. A. Zinn, U.S. patent 8,105,414 B2 (31 January 2012).
[18]H. J. Hwang, W. H. Chung, and H. S. Kim, Nanotechnology **23**(48), 485205 (2012).
[19]E. R. Dufresne, E. I. Corwin, N. A. Greenblatt, J. Ashmore, D. Y. Wang, A. D. Dinsmore, J. X. Cheng, X. S. Xie, J. W. Hutchinson, and D. A. Weitz, Phys. Rev. Lett. **91**(22), 224501 (2003).
[20]J. S. Kang, H. S. Kim, J. Ryu, H. T. Hahn, S. Jang, and J. W. Joung, J. Mater. Sci. Mater. Electron. **21**(11), 1213 (2010).
[21]W. P. Lee and A. F. Routh, Langmuir **20**(23), 9885 (2004).
[22]J. Jiang, G. Oberdörster, and P. Biswas, J. Nanopart. Res. **11**(1), 77 (2009).
[23]G. V. Franks and F. F. Lange, J. Am. Ceram. Soc. **79**(12), 3161 (1996).
[24]F. F. Lange and M. Metcalf, J. Am. Ceram. Soc. **66**(6), 398 (1983).
[25]K. L. Johnson, K. Kendall, and A. D. Roberts, Proc. R. Soc. London, Ser. A **324**(1558), 301–313 (1971).
[26]M. Yamamura, H. I. Ono, T. Uchinomiya, Y. Mawatari, and H. Kage, J. Chem. Eng. Jpn. **43**(2), 209 (2010).
[27]R. K. McGeary, J. Am. Ceram. Soc. **44**(10), 513 (1961).
[28]S. Tsantilis and S. E. Pratsinis, Langmuir **20**(14), 5933 (2004).
[29]J. H. Prosser, T. Brugarolas, S. Lee, A. J. Nolte, and D. Lee, Nano Lett. **12**(10), 5287 (2012).
[30]V. Subramanian, P. C. Chang, D. Huang, J. B. Lee, S. E. Molesa, D. R. Redinger, and S. K. Volkman, in *Proceedings of the 19th International Conference on VLSI Design* (2005), p. 1330.